IET Nanobiotechnology

Research Article

IET Journals
The Institution of Engineering and Technology

Synthesis of silver nanoparticles from a *Desmodium adscendens* extract and its antibacterial evaluation on wound dressing material

ISSN 1751-8741
Received on 12th April 2017
Revised 20th July 2017
Accepted on 6th August 2017
E-First on 18th September 2017
doi: 10.1049/iet-nbt.2017.0084
www.ietdl.org

Jaya R. Lakkakula[1,2] ✉, Derek Tantoh Ndinteh[3], Sandy F. van Vuuren[4], Denise K. Olivier[4,5], Rui W.M. Krause[1]

[1]*Department of Chemistry, Rhodes University, PO Box 94, Grahamstown 6140, South Africa*
[2]*Department of Bioscience and Bioengineering, IIT Bombay, Powai, Mumbai, India*
[3]*Centre for Nanomaterial Science Research, University of Johannesburg, PO Box 17011, Doornfontein, Johannesburg 2028, South Africa*
[4]*Department of Pharmacy and Pharmacology, University of the Witwatersrand, 7 York Rd, Parktown 2193, South Africa*
[5]*Department of Research and Development, Seda Essential Oils Business Incubator, 19 Mountain Street, Derdepoort 0186, South Africa*
✉ *E-mail: spencerjaya@gmail.com*

Abstract: The one-pot synthesis of silver nanoparticles (AgNPs) using the medium-polar extract of *Desmodium adscendens* (Sw.) DC. is presented here as an alternative synthesis of metal NPs. Characterisation of the formed NPs showed polydispersed AgNPs ranging from 15 to 100 nm where the concentration of metal ions was found to play a role in the size and shape of the prepared NPs. It could be established that the flavonoids, saponins, and alkaloids present in the extract acted as both reducing and stabilising agents during the formation of the capped metal NPs. This means of NP synthesis was also employed during the in situ immobilisation of AgNPs on gauze and plaster. An evaluation of the antibacterial activity of the medium-polar *D. adscendens* extract, AgNPs suspended in solution, and the immobilised AgNPs against *Staphylococcus aureus* (ATCC 25923), *Bacillus cereus* (ATCC 11778), and *Escherichia coli* (ATCC 25922) showed high efficacy against the latter in particular. This suggests that gauze, dilute silver nitrate solutions, and *D. adscendens* extract could be used successfully in the simple in situ preparation of effective antibacterial wound dressings.

1 Introduction

Traditional and herbal medicine remains the principal means by which significant segments of populations, especially in rural areas, ensure their physical and psychological well-being. An opportunity arises then to research a possibly symbiotic interaction between low cost, available traditional herbal medicines and efficient, scientifically viable modern materials.

Desmodium adscendens (Sw.) DC. was described by Hooker (1879) and is most commonly known as *Amor seco* [1, 2]. It is a weedy, perennial herb that grows to ~50 cm in height and produces numerous light-purple flowers followed by green fruits in small, beanlike pods. The species is indigenous to many tropical and subtropical areas such as the Amazon rainforest of Peru, in Brazil, as well as the West Coast and Central Africa [3]. *Desmodium adscendens* is popularly used as a medicinal plant for a wide range of indications among the native people in these countries. It is probably most well known for its potent anti-asthmatic properties and its use in treatment of diseases associated with smooth muscle contraction [4]. It is also used frequently in the treatment of wounds, stomach ailments, and other infections, where the leaves are used in most preparations as juice, infusions, or decoctions [2, 4]. In Brazil, for instance, it is used to treat leucorrhoea, body aches, pains, ovarian inflammations, excessive urination, gonorrhoea, and diarrhoea [5]. In African traditional medicine, Congolese healers use it to treat fever, pain, and epilepsy [6], while Cameroonians use it to prevent contracting respiratory infections [7]. In Ghana, leaf decoctions are popular as wound dressings and remedies for bronchial asthma, constipation, and dysentery [4]. With reference to the treatment of wounds, the leaves may be pounded, steeped in lemon juice, and bound on [8, 9], while with leprosy sores, smallpox, skin ailments, scabies, and itching, the affected areas may be washed with leaf extract [10, 11]. Venereal sores may be treated by bathing in leaf maceration [9, 12] or by drinking a decoction of leaves and stems [13]. Phytochemical investigation of the leaves [14–17] revealed the presence of triterpenoid saponins [e.g. dehydrosoyasaponin I (DHS-I), soyasaponin I, soyasaponin III, and astragalin], alkaloids such as tetrahydroisoquinolines (e.g. salsoline), *β*-phenylethylamines (e.g. tyramine and hordenine), and indole-3-alkyl amines [14, 15, 17] as well as phenolic compounds such as flavonoids (e.g. cosmosiin, tectorigenin, catechin, rutin, quercetrin glucosyl, and quercetrin dehydrate), anthocyanidins (e.g. cyanidin-3-*O*-sophoroside and pelargonidin-3-*O*-rhamnoside), and phenolic acids (e.g. gallic acid and cinnamic acid) (Fig. 1) [3, 4, 17].

Often rudimentary and simple preparations are used traditionally, especially in rural areas, for antibacterial treatment of wounds, possibly due to the lack of access to sterile wound dressings. Even in advanced scientific westernised procedures, there is a need for simple, less costly means of generating sterile wound dressings. To this effect, silver nanoparticles (AgNPs), in particular, have attracted considerable attention due to their diverse properties and uses, but also particularly due to their antimicrobial properties [18]. Research has resulted in various applications of Ag^+ and Ag^0, either in solution, ointments, or stationary on dressings, in the treatment of microbial infections consistent with burns and wounds [19]. While Ag^+ and Ag^0 have been effective in such treatments, bacteria, viruses, and fungi have shown some resistance against treatment with Ag [19] and that efficacy is dependent on dose levels as well as mode of microbial action [18]. To address such resistance, various capping and/or coating combinations are being investigated for these NPs. The antimicrobial properties of metal NPs are mostly attributed to their small sizes and corresponding large surface areas. In this instance, there have been many techniques reported in the literature for the synthesis of AgNPs of varying size and shape. Many of these methods are costly, require complicated laboratory set-ups, and almost always use or generate toxic materials. With these NPs widely applied in clinical treatments [20], more natural approaches for the

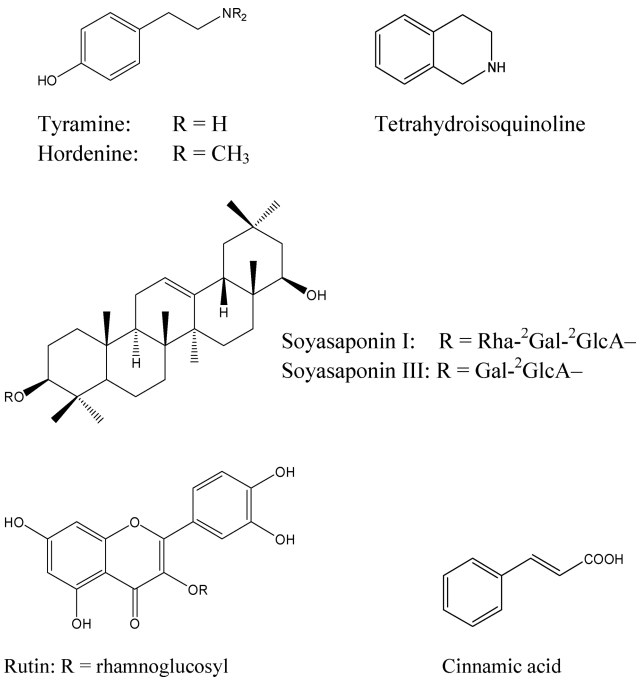

Fig. 1 *Examples of compounds isolated from D. adscendens*

development of nanobiomedicine are becoming viable options, and have led to interesting synthesis of metal NPs where microbes or plant extracts are being incorporated [21].

While the synthesis and in vitro antibacterial properties of AgNPs from *Desmodium triflorum* (L.) DC. were reported previously [22], the research reported here elaborates on the synthesis of AgNPs from whole plant medium-polar extracts of *D. adscendens* for the first time. The effect of variable concentrations of metal salts on the dimensions of the prepared NPs was also studied. As AgNPs are known to be efficient wound treatments, the rather unexplored in situ immobilisation of AgNPs was attempted using plaster and gauze dressings. Antibacterial studies were carried out with the *D. adscendens* extract, synthesised capped AgNPs, as well as the plaster and gauze dressings with immobilised AgNPs produced. The main aim with the results reported here is two-fold, i.e. to show effective metal NP-synthesis by using *D. adscendens* extract as both reducing and stabilising capping agent for AgNPs, and secondly, to explore cost-effective, simple yet effective in situ immobilisation of antimicrobial AgNPs on various wound dressings.

2 Materials and methods

2.1 Materials

A bulk whole-plant sample of *D. adscendens* was collected from Mount Eloumdem in the Centre Province of Cameroon and a voucher specimen deposited in the National Herbarium in Yaounde Cameroon (voucher number YA/41122/HNC).

Chloroform (CP, distilled before use) and methanol (AR) used for extraction were obtained from Merck. Silver nitrate ($AgNO_3$) (A.C.S. reagents) was obtained from Sigma-Aldrich. All aqueous solutions were prepared using deionised water.

Gauze, commercial plastic-backed plasters (ELASTOPLAST-AQUA PROTECT), and 'antibacterial plasters' (indicated on the packaging as being pre-coated with Ag ions) (ELASTOPLAST-ANTI BACTERIAL WATERPROOF) were obtained from a local pharmacy.

2.2 Preparation of plant extract

The whole plant sample (500 g) was air dried for 1 week and was finely ground with a commercial grinder. The ground material was then subjected to solvent extraction using chloroform/methanol (1 : 1). The mixtures were filtered, where after the organic filtrate was dried under vacuum to yield ca. 50 g crude extract. The crude organic extract was stored in an inert environment (4°C) until further use.

2.3 Preparation of AgNPs

Aqueous solutions (25 ml) of 0.5, 1, and 1.5 mM of $AgNO_3$ were reduced with 25 ml aliquots of *D. adscendens* plant extract each (2.5 mg extract reconstituted in 25 ml methanol), at room temperature [23] under continuous stirring. The $AgNO_3$ mixtures all changed to a red-brown colour, consistent with the formation of the corresponding AgNPs, within a period of 1 h. The solutions were left for 12 h to allow complete reduction in all metal ions. The reaction mixtures were consequently centrifuged at 1850*g* for 20 min to separate the formed NPs from the supernatant, where after the latter was discarded. The retained metal NP pellets were dispersed in water, washed three to four times, and dried.

2.4 Immobilisation of AgNPs on gauze, plaster, and antibacterial plaster

In each in situ preparation, the aqueous $AgNO_3$ solution, plant extract solution (in the same concentration combinations as above), and gauze, plaster, or antibacterial plaster (ca. 1×2 cm^2) were added to the respective reaction flasks simultaneously with continuous stirring. This allowed for the synthesis of AgNPs directly on the surface of the respective gauze, plaster, or antibacterial plaster. The mixtures were allowed to react for up to 120 h and AgNPs formation monitored at regular intervals (the liquors were analysed by means of UV–Vis) in order to monitor the formation of AgNPs, i.e. a decrease in Ag^+ concentration. The gauze and plasters were removed from the reaction medium, dried, and analysed by means of Fourier transform infrared (FTIR), scanning electron microscopy (SEM), energy dispersive absorption spectroscopy (EDS), and X-ray diffraction (XRD), where after the antibacterial activity of the treated gauze and plasters were determined.

2.5 Characterisation of AgNPs

The progress of AgNPs formation was observed by means of UV–Vis spectroscopy. The absorption spectra were recorded using a SHIMADZU UV-2540 spectrophotometer in the 200–900 nm range. FTIR spectra were obtained for the *D. adscendens* extract and synthesised NPs (both in powder form), as well as AgNPs immobilised on gauze and plasters by using a Perkin Elmer (FTIR

Spectrum 100) spectrophotometer in the spectral range of 4000–400 cm^{-1} with a resolution of 4 cm^{-1}. A ZnSe/diamond composite was used as the key component of the universal attenuated total reflectance sample holder. The transmission electron microscopy (TEM) analysis of the synthesised AgNPs was done under bright field by using a FEI Tecnai spirit G2 microscope at 120 kV. For this analysis, samples of the synthesised NPs were dispersed in acetone and sonicated for 10 min. A drop of this suspension was placed on the grid and excess sample was removed using blotting paper. SEM analysis was performed using an FEI Nova NanoSEM 200 to irradiate the immobilised AgNPs on the gauze and plasters with a beam of electrons at 15 kV. The elemental composition of the AgNPs was also determined in the process with the Genesis EDS attached to the SEM. In this instance, the samples were coated with Au through sputter deposition pre-treatment since Au is highly conductive and does not cause interferences with the EDS analysis of AgNPs. Lastly, powder XRD data was acquired by means of a Philips PANalytical X'pert PRO diffractometer operated at 40 kV and 40 mA. The Cu $K\alpha_1$ radiation beam ($\lambda = 0.15406$ nm) [Ni filtered (0.02 mm) and masked (11.6 mm)] was collimated with Soller slits (0.04 rad). Measurements were performed in the range of 20–100° (2θ). Samples of gauze and plasters with immobilised AgNPs were pressed into pellets and mounted on a sample holder using a bracketed sample stage. Data analysis was evaluated using X'pert data collector software.

2.6 Antimicrobial evaluation

2.6.1 Desmodium adscendens extract and synthesised AgNPs: Minimum inhibitory concentration (MIC, defined as the lowest concentration at which microbial growth is inhibited) values were determined using the microtitre plate method [24, 25]. Results were obtained in duplicate (or triplicate where duplicate results were not congruent) for each bacterial strain. The bacteria [*Staphylococcus aureus* (ATCC 25923), *Escherichia coli* (ATCC 25922), and *Bacillus cereus* (ATCC 11778)] were subcultured from stock Tryptone Soya agar (TSA) plates and grown at 37°C in Tryptone Soya broth (TSB) overnight. Distilled sterile water (100 µl) was placed into each of the 96 wells of an aseptically prepared microtitre plate. The dried AgNPs were reconstituted in distilled sterile water and the *D. adscendens* extract in acetone to afford starting concentration of 1 mg/ml for both mixtures. These mixtures were subsequently transferred into the first row of the microtitre plate and doubling serial dilutions were performed. The stock cultures of the three bacteria strains were diluted in TSB and standardised to a 0.5 McFarland standard (approximate inoculum size of 1×10^6 CFU/ml). These diluted bacterial solutions (100 µl) were added to each of the wells of the microtitre plates. Sterile water and acetone were included as negative controls, and ciprofloxacin as the positive control (to confirm antimicrobial susceptibility) at a starting stock concentration of 0.01 mg/ml. The microtitre plates were consequently covered with sterile seals and incubated overnight at 37°C to stimulate bacterial growth. After incubation, 40 µl of a 0.2 mg/ml *p*-iodonitrotetrazolium violet solution was added to each well and left to stand for 6 h. The plates were examined for bacterial growth, indicated by the appearance of a red/pink colour in the well. The MIC was determined by the lowest concentration at which there is no bacterial growth.

2.6.2 AgNPs-coated gauze, plaster, and antibacterial plaster: The antibacterial efficacy was evaluated by means of the disc diffusion assay against *E. coli* (ATCC 25922) [26]. Petri dishes with TSA were prepared with an inoculum of *E. coli* equivalent to a 0.5 McFarland standard. The AgNP-loaded materials, i.e. gauze, plaster, and antibacterial plaster (three replicates for each type of material, from each concentration combination of $AgNO_3$ with extract), were cut into appropriate sizes (5 × 5 mm) and placed aseptically on the agar surface. A control disc of commercially available ciprofloxacin at 5 µg concentration (Oxoid) was used as a positive control. The petri dishes were incubated for 24 h after which the zones of inhibition were measured and the activity determined based on the width of the zones (in mm, from the edge of the ciprofloxacin wafer, gauze, or plaster sample to the edge of the zone of inhibition) in which the growth of bacteria was inhibited around the disc. Only *E. coli* was used as a pilot study aimed to ascertain whether the antibacterial properties of AgNPs immobilised in situ on gauze, plaster, and antibacterial plaster were maintained and comparable to the activities exhibited by the AgNPs synthesised in solution with *D. adscendens*. It was also useful to determine the actual size of the sterile zone around the materials on the TSA resulting from bacterial growth inhibition under these conditions in order to evaluate the practical applicability of this study.

3 Results

3.1 Synthesis of AgNPs using D. adscendens extract as reducing agent

When comparing the UV–Vis spectrum (Fig. 2) of the *D. adscendens* extract with those obtained for the AgNPs, the former shows an intense peak with a shoulder between 250 and 350 nm confirming the presence of simple unconjugated phenylalkylamines (expected at 260–280 nm) and tetrahydroisoquinolines (maximum at ∼285 nm) [27], as well as flavonoids such as tectorigenin, quercetrin, and rutin (maxima expected at ∼260 and 360 nm) [28]. These peaks are less intense and no shoulder is visible at 325 nm with the Ag^+ mixtures (0.5, 1.0, and 1.5 mM), indicating that the phenolic characters of the mentioned compounds have been changed. Typically, for the AgNP solutions, similar strong broad peaks were observed at 420 nm, despite a variation in molar concentrations (0.5, 1, and 1.5 mM) of the $AgNO_3$ solutions when introduced. FTIR spectra were obtained for the *D. adscendens* extract and all the AgNPs synthesised (Fig. 3) to identify the major classes of compounds in the extract possibly responsible for the bio-reduction, capping, and efficient stabilisation of the metal NPs. The band at 1020 cm^{-1} (Fig. 3*a*) observed for the extract is typical of –C–O– linkages present in ethers and polyols, i.e. flavonoids or saponins. The presence of alkaloids were confirmed with the bands at 3318 cm^{-1} (–N–H stretches) and 1020 cm^{-1} for –N–C– stretching vibrations of aromatic and aliphatic amines, respectively [23, 29]. When comparing the spectra of the extract with that of the AgNPs (Fig. 3*b*), the band at 3318 cm^{-1} broadened and became more intense at 3326 cm^{-1} further corresponding with the stretching frequency of hydrogen-bonded alcohols and primary amines. Also, a band is observed at 1639 cm^{-1} (Fig. 3*b*) which corresponds with the bending frequency for primary amines or carbonyl carbon moieties from ketones or carboxylic acids. While the disappearance of the band at 1020 cm^{-1} (Fig. 3*a*) indicates oxidation of the N-containing functionalities, the remaining bands between 1000 and 1400 cm^{-1} (–N–C– stretching vibrations) also confirm the presence of amines on the AgNPs surface.

Where size and shape of the formed AgNPs are concerned, the NPs seem to be small (sizes ranged from 15 to 100 nm, according to the TEM results; Figs. 4*a–c*) and spherical, typically found with AgNPs synthesised from plant extracts [21]. It was further observed that a larger quantity of AgNPs is formed at the higher concentration (1.5 mM $AgNO_3$), the particle size distribution is narrower, and the particles are the smallest as plotted in size distribution histogram in Figs. 4*d–f*.

3.2 Immobilised AgNPs prepared in situ on gauze and plasters

The formation of AgNPs in solution was monitored (using UV–Vis, Figs. 5*a–c*) as an indication of complete formation of immobilised AgNPs on the gauze and plasters. Again, as 0.5, 1, and 1.5 mM $AgNO_3$ solutions were reduced with extracts of the same concentration (1 mg/10 ml methanol), colour changes from greenish to light reddish-brown were observed, where the UV spectra exhibited the characteristic AgNPs strong broad SPR peak at 420 nm. As reaction time increased, the peak intensity increased and the shoulders on the peaks became smaller. The elimination of

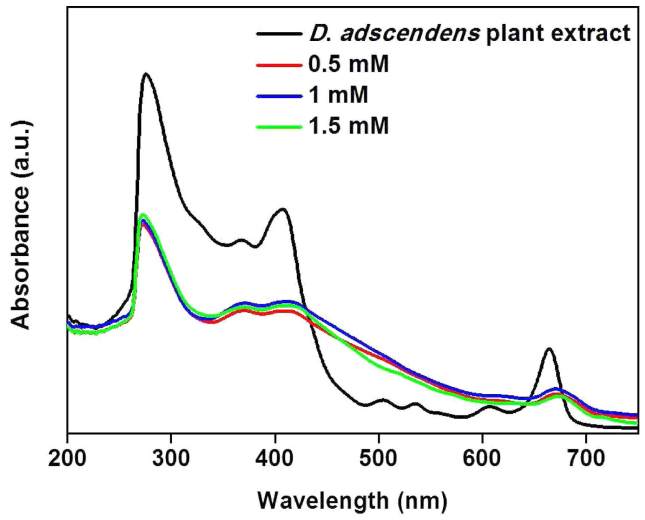

Fig. 2 *UV–visible spectra of D. adscendens plant extract and SPR peaks when the extract is treated with different concentrations of $AgNO_3$ (0.5, 1.0, and 1.5 mM) after 12 h*

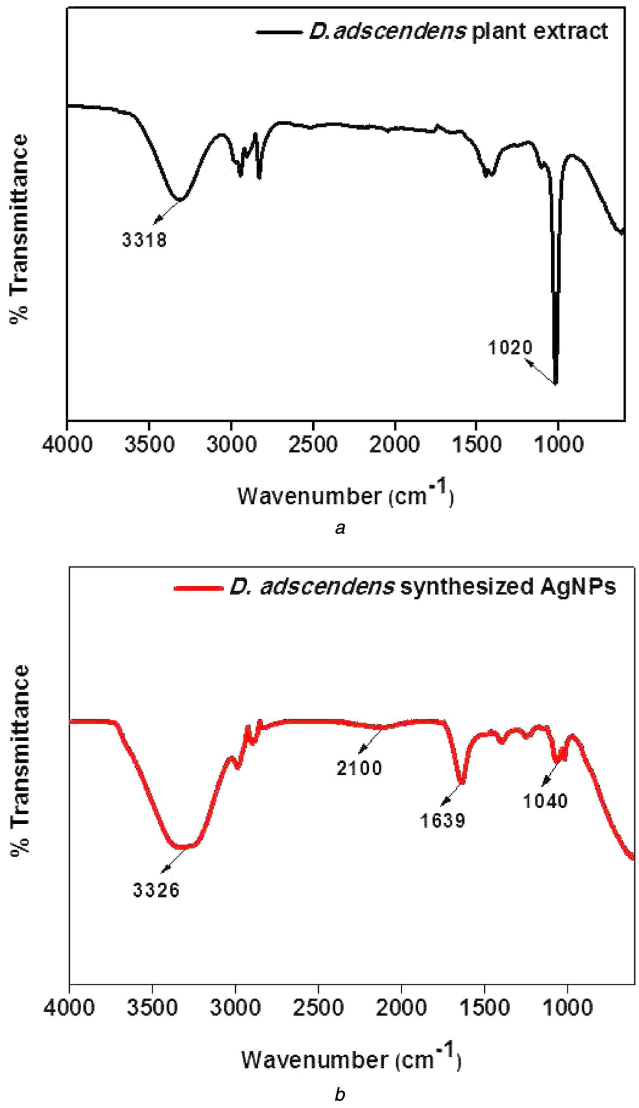

Fig. 3 *FTIR spectra of*
(a) *Desmodium adscendens* leaf extract, ***(b)*** Synthesised AgNPs

the shoulder on the 420 nm peak was fastest with the use of antibacterial plaster.

The FTIR spectra of immobilised AgNPs were comparable to those of the AgNPs in solution (Figs. 3 and 5*d–f*). It was observed that the bands at 3328, 3365, and 3427 cm^{-1} for the treated gauze, plaster, and antibacterial plaster, respectively, were not present with untreated gauze and plaster. These bands, typical of –N–H and –O–H stretching, confirm the presence of AgNPs on the gauze and plaster.

From the SEM images (Figs. 6*a–l*), well-dispersed AgNPs are visible on the various gauze and plasters irrespective of the concentration of $AgNO_3$ used. It is also evident that the particle size increases with increased concentration, and the particles formed from the 0.5 mM Ag^+ solutions are so small that they are considered crystalline (according to the XRD results – Fig. 7). The largest particles were formed on the antibacterial plaster (Figs. 6*j–l*) in comparison with the gauze and normal plaster. Confirmation of the successful reduction in Ag^+ to elemental Ag^0 on the gauze and plasters was accomplished through EDS analysis where an intense signal at 3 keV is indicative of the elemental silver [22] (Fig. S1).

The XRD patterns of the untreated gauze and plasters were compared with those where immobilised AgNPs were synthesised from 0.5 mM $AgNO_3$ since these particles were the smallest and thus expected to be crystalline (Figs. 7*a–f*). A number of Bragg reflections with 2θ values for sets of lattice planes were observed (Table 1). The resulting 2θ diffractions, respectively, indexed to the [111], [200], [220], and [311] planes, are typical of face-centred cubic (fcc) silver nanocrystals, with unassigned Bragg peaks at reflections [222] and [400] [29].

3.3 Antimicrobial properties of synthesised and immobilised AgNPs

From the MIC results (Table 2), it is evident that the plant extract is only moderately active [30], whereas the AgNPs prepared from it, all exhibit significant activity, i.e. MIC values for compounds reported below 1 mg/ml and even lower (≤16 µg/ml), are considered noteworthy [31–33]. The best overall activity was observed for B. *cereus* (2.50–12.50 µg/ml), where the size–activity relationship was most pronounced with *E. coli,* i.e. the smallest AgNPs (10–20 nm) exhibited the best activity (MIC of 0.25 µg/ml), comparable to that of the positive control (ciprofloxacin, MIC of 0.16 µg/ml). Particles sized 10–50 nm exhibited the best activity against *S. aureus* (7.80 µg/ml). Where the results for the *E. coli* disc diffusion assays are concerned, it was evident that the gauze with immobilised AgNPs exhibited the best activity (zones of inhibition: 2–5 mm – Table 3).

4 Discussion

Iravani [21] reviewed the green synthesis of metal NPs by using plant extracts as one of many avenues for such synthesis. Of the ca. 70 reports reviewed, variation in several factors during synthesis of AgNPs, such as the type of plant extract, concentrations of extract and metal salt solutions, pH, and temperature, resulted in different morphologies and dispersities of the formed NPs. However, all the reported synthesis reactions were completed rapidly (in <24 h), and the resulting capped NPs were stable in solution for long periods, as was also the case here. With metal NPs, the distinctive reddish-brown colour for the AgNPs is due to surface plasmon resonance (SPR) which is measured by means of UV–Vis as peaks [34]. The position and shape of plasmon absorption peaks are strongly dependent on the particle shape and size, as well as the dielectric constant of the surface adsorbed species and, to a smaller extent also that of the solvent used [35]. Pandey *et al.* [36] have previously examined the relationship between SPR-generated peaks of AgNPs, NP-morphology, and pH where an increase in peak intensity indicates enhancement in the rate of formation of AgNPs or the amount of NPs formed. The sharpness of the peak relates to dispersity and the shift to the red or blue regions of the spectra is indicative of the relative sizes of the formed particles. Based on these criteria, it was evident that the strong broad peaks at 420 nm observed for all the reaction mixtures, typical of AgNPs [23], indicated large yields of polydispersed NPs [36]. A general trend where higher yields of NPs seem to be produced from lower concentrations of metal ions has been reported [37], but cannot be

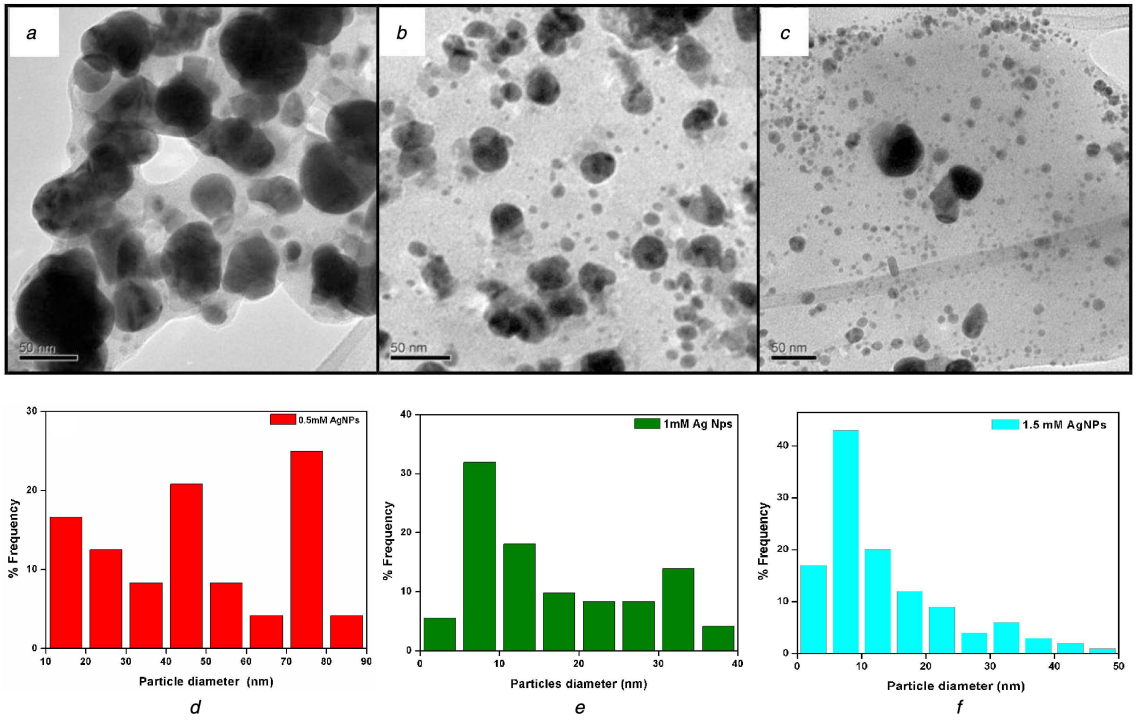

Fig. 4 *AgNPs at different concentrations of Ag ions*
(a) TEM image at 0.5 mM, ***(b)*** TEM image at 1.0 mM, ***(c)*** TEM image at 1.5 mM, ***(d)*** size distribution at 0.5 mM, ***(e)*** size distribution at 1.0 mM, ***(f)*** size distribution at 1.5 mM

superimposed on all NP syntheses since Gurunathan *et al.* [38] reported observations where, with varying $AgNO_3$ concentrations from 1 to 10 mM, there was an increase in yield from 1 to 5 mM, but a decrease between 6 and 10 mM. Furthermore, with lower concentrations of metal ions in relation to extract, it would be possible to produce smaller NPs since the biomolecules in the extract responsible for reducing and stabilising the NPs through capping could cause enhanced repulsion between the formed NPs, resisting agglomeration, and consequently lead to the formation of smaller NPs [34]. The contrary is observed from our results where 1.5 mM $AgNO_3$ afforded the smallest (10–20 nm) particles with the smallest size distribution. Consequently, metal ion concentration is a variable that should be optimised for each unique set of reagents. The shoulder observed at 370 nm in the UV–Vis spectra of the synthesised AgNPs (Figs. 2 and 5) is suggested to correspond to the transverse plasmon vibration in the AgNPs whereas the peak at 440 nm is due to excitation of longitudinal plasmon vibrations. The distinct separation of 70 nm between these wavelengths is said to indicate that the AgNPs are assembled into open, quasilinear superstructures in solution [39].

Compounds with carboxylic (–COOH), hydroxyl (–OH), and amine ($–NR_3$) moieties (i.e. the saponins, flavonoids, and alkaloids in the *D. adscendens* extracts) are particularly known to not only reduce metal ions [21], but also cap and stabilise metal NPs [33].

These functionalities are present in the three major classes of compounds, i.e. phenolic compounds, alkaloids and saponins, as have been shown by various authors [40, 41]. The leaves reportedly contain mainly flavonoids compounds [12.8 mg (catechin equivalent)/g dry weight] and polyphenol compounds [11.1 mg (gallic acid equivalent)/g dry weight, with anthocyanins [0.0182 mg (cyanidin-3-glucoside equivalents)/g dry weight], and tannins [0.39 mg (catechin equivalent)/g dry weight] as minor constituents. Muanda *et al.* [40] revealed the main phenolic compound in the methanol–water leaf extract as quercetrin dihydrat (2.11 mg/ml), where Baiocchi *et al.* [41] identified 4 related soyasaponins, 4 simple alkaloids, and 35 different flavonoids (mainly apigenin and kaempherol glycosylated derivatives) from the leaves. Based on these results, it can be deduced that the phenolic component of the extract would have played a major role, with a smaller contribution being made by the alkaloids and saponins present. The main reason for this is the relative solubility of the latter two classes of compounds in medium-polar solvents during extraction, where saponins are only slightly soluble in medium-polar extracts due to their extensive glycosylation, and most alkaloids become available in extracts upon prior acid–base extraction, which was not done in this instance [41].

The presence of these compounds in the medium-polar *D. adscendens* extract was confirmed by means of FTIR (Fig. 3). When comparing the FTIR spectra of the extract with that of the AgNPs (Fig. 3*b*), the band at 3318 cm^{-1} broadened and became more intense at 3326 cm^{-1} corresponding with the stretching frequency of hydrogen-bonded alcohols and primary amines. Hydrogen bonding may consequently be a means of stabilisation exerted by the compounds in the extract during the formation of the AgNPs. The disappearance of the band at 1020 cm^{-1} (extract, Fig. 3*a*) in Fig. 3*b* (AgNPs) possibly indicates the bio-reduction of Ag^+ to Ag^0 and consequent oxidation of some of the primary or secondary hydroxyl groups present in the flavonoids or saponins. The –N–C– stretching vibrations on the AgNP surface also confirm the presence of amines, further contributing to the stabilisation of the NPs [23]. The stabilisation of metal NPs produced from plant extracts has been attributed to the presence of proteins in many instances, resulting in the observation of amide bands in the FTIR spectrum [21], as was also reported for AgNPs obtained using an aqueous extract of *D. triflorum* [22]. Proteins were, however, not considered present in the MeOH/chloroform plant extract used in this study since proteins are known to precipitate from solvents with similar or lower polarity than 75% ethanol in water (i.e. proteins, polysaccharides, and glycolipids are alcohol precipitable solids) [42].

Where pH of the reaction medium is concerned, it was reported that a neutral to basic pH results in the highest yields of spherical (rather than ellipsoidal) AgNPs with the smallest size distributions (typically 6–100 nm) when plant extracts are used as reducing agents [36, 43, 44]. For this study, pH as a variable was not investigated, since weakly basic alkaloids were present in the extract solution, making the reaction medium pH conducive to formation of small, mostly spherical AgNPs (sizes ranged from 15 to 100 nm, as according to the TEM results; Fig. 4).

Several approaches may be followed to immobilise NPs on textiles without the use of synthetic chemical reducing agents and/or stabilisers [37]. The method followed here was adapted from an in situ reduction in metal salts by means of the aldehyde

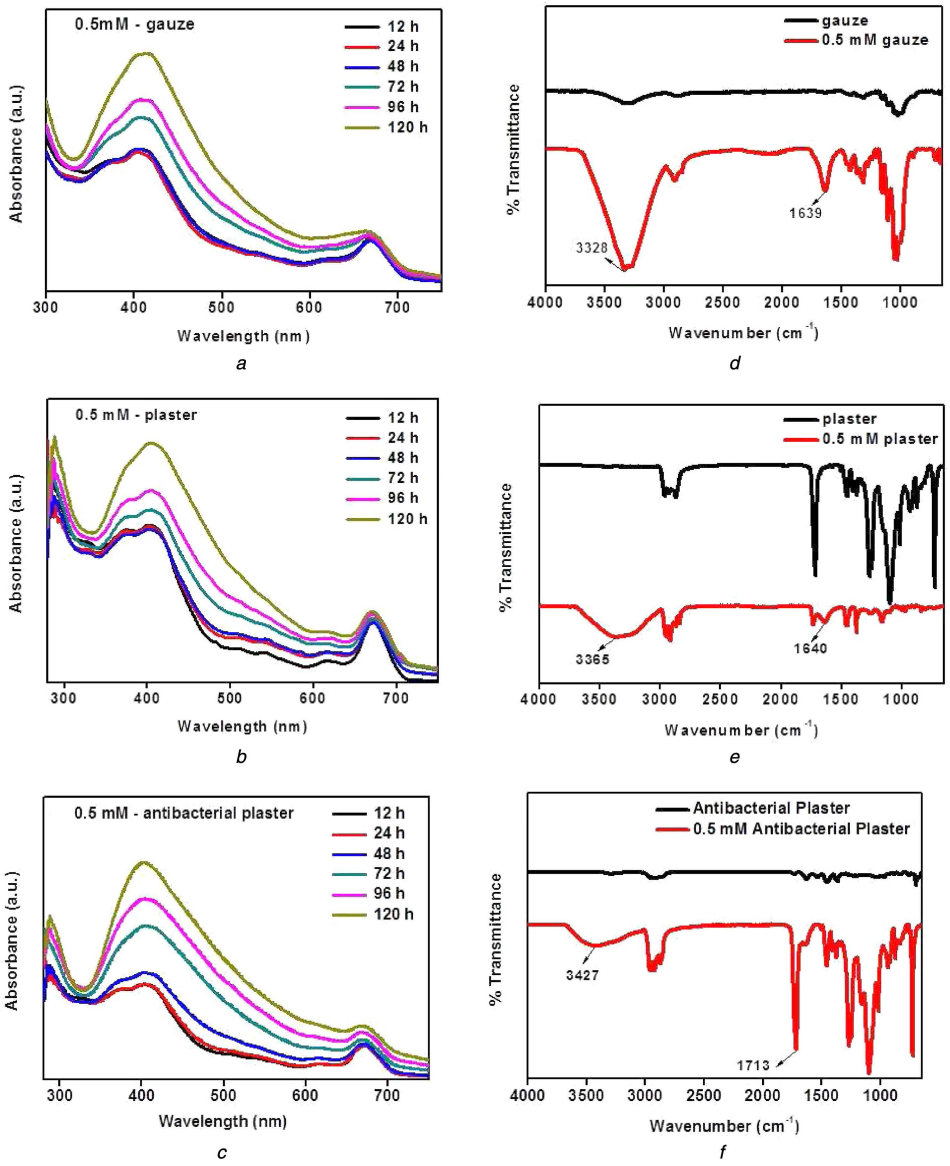

Fig. 5 *UV–Vis monitored bioreduction of Ag^+ (0.5 mM $AgNO_3$) to Ag^0 over a period of 120 h, on*

(a) Gauze, ***(b)*** Plaster, ***(c)*** Antibacterial plaster using *D. adscendens* plant extract; FTIR monitored bioreduction of Ag^+ (0.5 mM $AgNO_3$) to Ag^0, on ***(d)*** Gauze, ***(e)*** Plaster, ***(f)*** Antibacterial plaster

functionalities present in starch (gauze and plasters), where the latter also provided stabilisation of the formed AgNPs on the gauze and plasters added to the reaction mixture [44]. From the UV–Vis results (Fig. 5), it could be observed that the SPR peak intensity increased as the NP concentration increased, and the shoulders on the peaks became smaller as the capping compounds on the surfaces of the NPs were oxidised [35, 36]. This effect was most pronounced with antibacterial plaster due to the presence of already impregnated Ag^+ ions on the plaster, suggesting that the increased concentration of Ag^+ (already on the plaster as specified on the packaging, combined with $AgNO_3$ in the reaction medium) enhanced the rate of oxidation of the capping compounds. The FTIR spectra of immobilised AgNPs were comparable to those of the AgNPs in solution, also supporting the stabilisation of the immobilised AgNPs through hydrogen bonding of flavonoids, saponins, and alkaloids in the extract. In this instance, it should also be noted that cotton, often used in gauze and plasters, is a natural fibre consisting of cellulose with repeating β-1,4 linked D-glucose units. Cellulose itself has an extensive surface area which implies that a cotton fibre will have many protruding hydroxyl moieties on its surface which would further facilitate adsorption and stabilisation of AgNPs quite efficiently [44]. From the SEM images (Figs. 6*a–l*), it was evident that the particle size increased with increased concentration of $AgNO_3$. This trend is consistent with that reported by Ravindra *et al.* [44]. The largest particles were formed on the antibacterial plaster due to the fact that this reaction medium contained increased concentrations of Ag^+. These observations show that the already immobilised Ag^+ ions were reduced through contact with the plant extract and then acted as 'seeds' around which the AgNPs continued growing [45]. The XRD patterns of the immobilised AgNPs confirmed the presence of crystalline fcc silver nanocrystals [29, 44], as also observed for those prepared using *D. triflorum* [22]. The unassigned Bragg peaks at reflections [222] and [400] might have resulted from the extract molecules capping and stabilising the nanoparticles [29].

In the research presented here, the three strains of bacteria associated with infected wounds, i.e. *E. coli* (Gram-negative) as well as *S. aureus* and *B. cereus* (both Gram-positive), have been exposed to solutions containing AgNPs of different sizes prepared from a medium-polar *D. adscendens* extract, where the latter is also known to be used for the treatment of wounds. While *S. aureus* is commonly associated with wound infections, *E. coli* and *B. cereus* are normally associated with gastrointestinal infections. The latter two strains have however been incorporated in this study as they are also associated with surgical wounds [46, 47]. Furthermore, the effect of the synthesised and immobilised AgNPs on both Gram-negative and Gram-positive bacteria could indicate a possible mode of action. AgNPs exhibit a wide range of

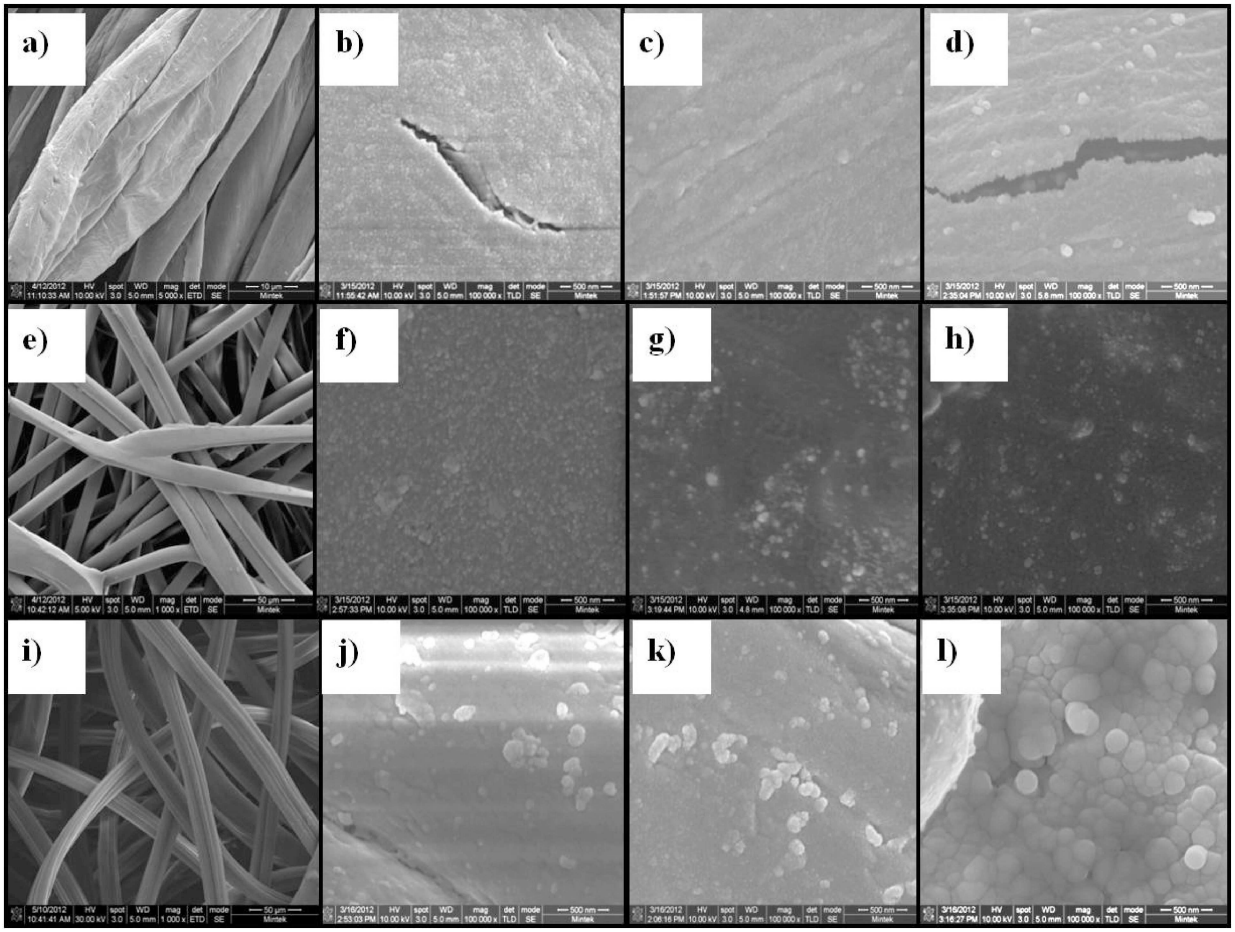

Fig. 6 *SEM images of*

(a) Plain gauze; AgNPs on gauze synthesised from $AgNO_3$ solutions of ***(b)*** 0.5 mM, ***(c)*** 1 mM, ***(d)*** 1.5 mM with *D. adscendens* extract; ***(e)*** Plaster; AgNPs on plaster synthesised from $AgNO_3$ solutions of ***(f)*** 0.5 mM, ***(g)*** 1 mM, ***(h)*** 1.5 mM; ***(i)*** antibacterial plaster; AgNPs on antibacterial plaster synthesised from $AgNO_3$ solutions of ***(j)*** 0.5 mM, ***(k)*** 1 mM, and ***(l)*** 1.5 mM with *D. adscendens* extract. [Magnification of (*a*), (*e*) and (*i*) – 50 μm; magnification of all other photos – 500 nm]

antimicrobial effects through multiple biochemical pathways. Two major bactericidal mechanisms are suggested, i.e. firstly through direct nanomechanical action via the attachment of the NPs to the bacterial cell membrane where important functions such as permeability, electron transport, and respiration, are disturbed, or secondly, through AgNPs permeation and accumulation inside the bacteria where it interferes with the metabolic and growth signalling pathways by means of the (delayed) release of Ag^+ ions from the AgNPs. The ions then accumulate intracellularly affecting DNA replication and ATP production [18, 48, 49]. The nanomechanical bactericidal efficacy of metal NPs is thus dependent on size, shape, concentration as well as the surface charge density, and chemical properties of the metal NPs determined by the capping agents present [50, 51]. In this instance, smaller AgNPs (up to 80 nm in diameter) are able to permeate the cell membrane, and a larger exposure to capping agents affected by larger surface areas play a role in the successful initial attachment of the AgNPs to anchoring sites on the cell membrane [50]. In this instance, the size–activity relationship was observed to be most pronounced with *E. coli,* where the smallest AgNPs exhibited the best activity, comparable to that of the positive control. In this instance, the smallest particles will have the largest surface area, and will thus provide the most reaction sites together with the ability to penetrate bacterial cells more efficiently. High inhibition observed for *E. coli* possibly also indicates that the negatively charged bacterial surface contributes to the sequestration of free Ag^+ ions which enters the cell through a damaged cell membrane [48, 49]. Once the AgNPs have entered the cell, Ag^+ is also released when AgNPs are subjected to oxidative metabolic processes within the cell, thus enhancing the activity [22]. In this instance, replication of DNA molecules is effectively conducted only when DNA molecules are in a relaxed state. With interference from the sequestrated Ag^+, the DNA molecules condense so that the replicating ability of the cell is lost [48, 49]. Another possible antibacterial mechanism affected by Ag^+ is through an interaction with thiol groups in proteins whereby the enzyme activity within the cell is inactivated [48]. The overall damage to the *E. coli* cells not only prevents division, but also leads to cell death. AgNP penetration into the cell, however, is not the only mechanism through which bactericidal activity is effected since the best overall activity was reported for *B. cereus*, and the peptidoglycan in the cell walls of Gram-positive (*S. aureus* and *B. cereus*) cells is much thicker than that in the Gram-negative *E. coli*, so that the thicker cell wall protects the cell from penetration of Ag^+ into the cytoplasm. In this instance, Taglietti *et al.* [49] reported large electron-dense aggregates (AgNPs) surrounded by biological material on the cell surface of *S. aureus* (observed in TEM images) where this phenomenon was observed less frequently in *E. coli* samples (since the AgNPs are able to penetrate this bacteria). Also, visual precipitation was reported after 24 h of incubation in *S. aureus* cultures when the concentration of AgNPs was sufficiently high to produce macroscopic effects. Since AgNPs themselves are soluble, dispersed, and stable at the pH of the culture broth (pH = 7), the precipitation and the aggregation observed were suggested to be produced by the interaction of the NPs with biological material. The latter may very well be proteins since silver is known to cause the deposition of proteins in vitro [48]. Interestingly, the formation of these AgNP aggregates might not lead to cell damage, but does prevent cell division [49], so that the MIC results reported here for the Gram-positive strains may be ascribed to a bacteriostatic effect rather than being bacteriocidal. This effect may be the major contributing mechanistic pathway where *S. aureus* is concerned in this study, where it was observed that the larger particles presented better MIC values. The quantity of Ag^+ on the

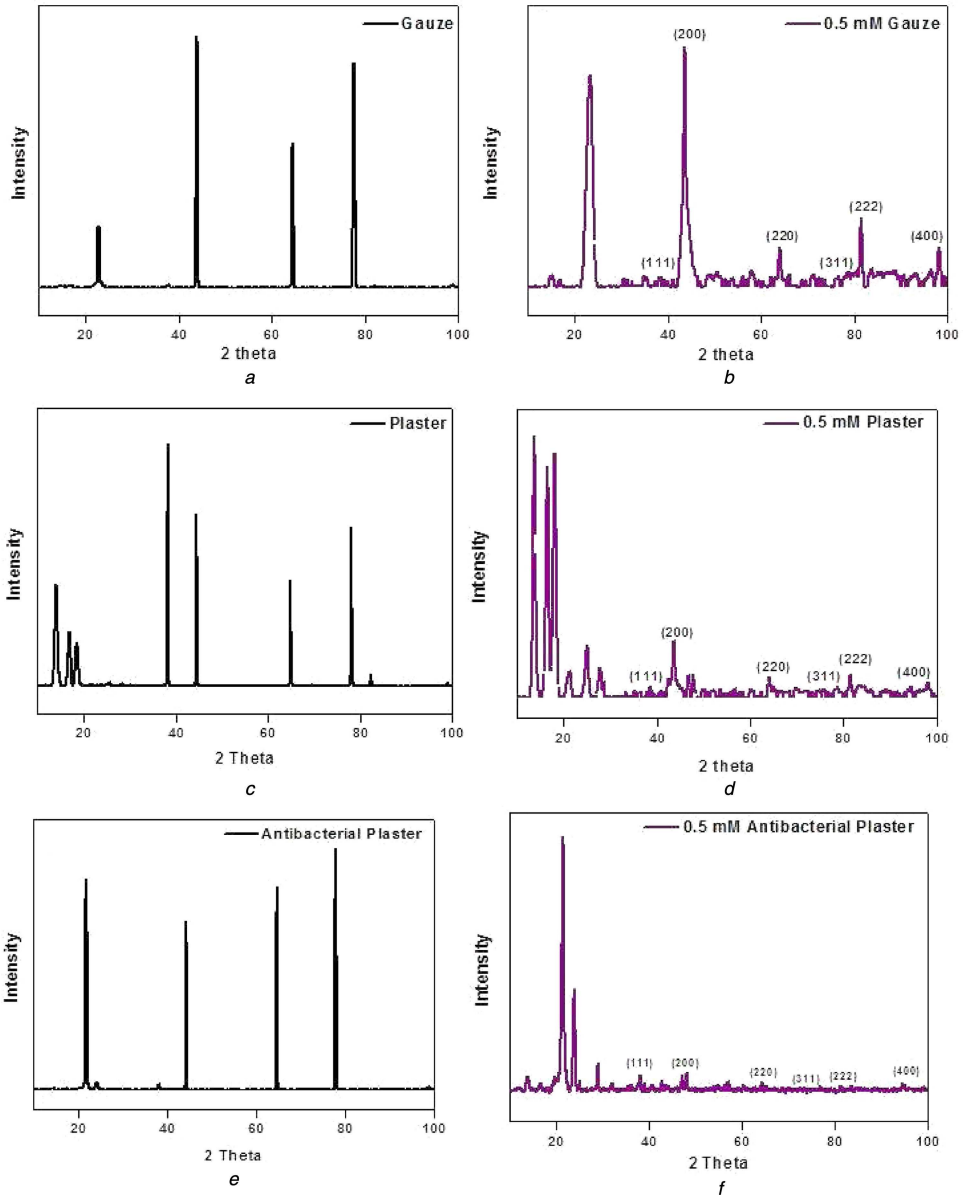

Fig. 7 *XRD spectra of untreated*

(a) Gauze, ***(c)*** Plaster, ***(e)*** Antibacterial plaster; XRD spectra of ***(b)*** Gauze, ***(d)*** Plaster, ***(f)*** Antibacterial plaster treated with 0.5 mM $AgNO_3$ and plant extract to form immobilised capped AgNPs

Table 1 XRD diffraction peaks for synthesised AgNPs on gauze, plaster, and antibacterial plaster obtained using 0.5 mM $AgNO_3$ and *D. adscendens* extract

Fibre samples treated with 0.5 mM $AgNO_3$	Diffraction peaks at various reflections, deg					
	111	200	220	311	222	400
gauze	38.20	43.64	64.00	76.25	81.46	98.14
plaster	38.62	43.63	63.97	77.90	81.47	98.14
antibacterial plaster	38.14	43.66	64.38	76.78	81.37	99.01

surface of the cells could consequently have caused more extensive agglomeration. With *B. cereus*, it is possible that both internal disruptive and nanomechanical mechanisms could have played a role since good activity was observed with all sizes of particles.

With the *E. coli* disc diffusion assays, the gauze with immobilised AgNPs exhibited the best activity, also due to the fact that it contained the smallest immobilised AgNPs when compared with those on the plaster and antibacterial plaster (Fig. 6). The results presented here not only compare well with those reported for *E. coli* and *S. aureus* where plant extracts were employed as reducing agents in the synthesis of immobilised AgNPs on cotton [40] but also indicate that these synthesised AgNPs could be a potent antimicrobial agents in the treatment of a variety of wound infections. However, it should be noted that only nanomechanical mechanisms of action as described above will be applicable with these immobilised AgNPs so that less efficient antibacterial activity might be a consequence of the restriction of translational freedom of the AgNPs, limiting penetration into *E. coli* cytoplasm [49].

5 Conclusions

Phytosynthesis of AgNPs using *D. adscendens* plant extract yielded spherical AgNPs where the concentration of Ag^+ played a role in the size distribution of the metal NPs obtained. It was evident that saponins, alkaloids, and phenolic compounds acted as reducing and stabilising capping agents. Furthermore, the

Table 2 MIC data for *D. adscendens* extract, synthesised capped AgNPs (presented in µg/ml)

Samples	Concentration $AgNO_3$, mM	NP size distribution, nm	*E. coli*[a] (ATCC-25922)	*B. cereus*[b] (ATCC-11778)	*S. aureus*[b] (ATCC-25923)
D. adscendens extract			2000	2000	2000
AgNPs	0.5	10–100	62.50	2.50	15.00
	1	10–50	31.30	12.50	7.80
	1.5	10–20	0.25	2.50	125.00
positive control					
ciprofloxacin			0.16	0.31	0.31
negative controls					
culture			>16,000	>16,000	>16,000
water			>16,000	>16,000	>16,000
acetone			>16,000	2000	>16,000

[a]Gram-negative strain.

[b]Gram-positive strain.

Table 3 Mean zones of inhibition obtained through disc diffusion assay for (i) gauze, (ii) plaster, and (iii) antibacterial plaster with immobilised capped AgNPs against *E. coli*

Samples with AgNPs	Concentration $AgNO_3$, mM	Zone of inhibition, mm[a]
gauze	0.5	5
	1.0	2
	1.5	4
plaster	0.5	3
	1.0	3
	1.5	3
antibacterial plaster	0.5	2
	1.0	2
	1.5	2
positive control		
ciprofloxacin (5 µg)		8

[a]Mean of three replicates, measured from edge of disc/sample to edge of zone.

pronounced bactericidal efficacy of smaller AgNPs against *E. coli, B. cereus*, and *S. aureus* were shown whether the NPs were in solution or immobilised on gauze or plaster. The main advantage of these findings lies in the simplistic approach for the preparation of metal NPs together with the proven applicability of AgNPs in the sanitation of wounds. These NPs are stable over long periods of time where the capping extract molecules not only afford the prevention of agglomeration and aggregation of the NPs which would cause a decrease in surface area, but also contributes to the retarded release of Ag^+ ions in aqueous solutions. This in turn affords prolonged antibacterial activity and a decrease in resistance caused by excessive Ag^+ ion dosages. Since the synthesis of AgNPs using plant extracts is so simple and inexpensive, it could become an affordable means to manufacture highly effective, stable wound-treatments in any laboratory where good laboratory and manufacturing practices may be implemented, even in impoverished countries.

6 Acknowledgments

The authors thank Mr. Fanuel Mokae at MINTEK for SEM analysis, Prof. Alexander Ziegler at University of Witswatersrand for TEM analysis, as well as Rhodes University for funding the project.

References

[1] Hooker, J.D.: '*Flora of British India*', vol. **2** (L. Reeve & Co. Ltd, England, 1879), p. 169

[2] Taylor, L.: 'Update on Amor Seco (*Desmodium adscendens*)', 2013. Available at http://www.rain-tree.com/amorseco.htm#.UvnqIq_xsaI, retrieved 11 February 2014

[3] Muanda, F.N., Bouayed, J., Djilani, A., *et al.*: 'Chemical composition and cellular evaluation of the antioxidant activity of *Desmodium adscendens* leaves'. ECAM 2011, 2010

[4] Rastogi, S., Pandey, M.M., Rawat, A.K.S.: 'An ethnomedicinal, phytochemical and pharmacological profile of *Desmodium gangeticum* (L.) DC. and *Desmodium adscendens* (Sw.) DC', *J. Ethnopharmacol.*, 2011, **136**, (2), pp. 283–296

[5] Guarin, G.: 'Plantas medicinais do Estado do Mato Grosso'. ABEAS 31, 1996

[6] N'gouemo, P., Baldy-Moulinier, M.B., Nguemby-Bina, C.: 'Effects of an ethanolic extract of *Desmodium adscendens* on central nervous system in rodents', *J. Ethnopharmacol.*, 1996, **52**, (2), pp. 77–83

[7] Sandberg, F., Perera-Ivarsson, P., El-Seedi, H.R.: 'A Swedish collection of medicinal plants from Cameroon', *J. Ethnopharmacol.*, 2005, **102**, (3), pp. 336–343

[8] Burkill, H.M.: '*The useful plants of West Tropical Africa*', vol. **3** (Royal Botanical Gardens, Kew)

[9] Neuwinger, H.D. (Ed.): '*African traditional medicine – a dictionary of plant use and applications*' (Medpharm Scientific Publishers, Stuttgart, 2000), p. 172

[10] Bouquet, A., Debray, M.: '*Plantes médicinales de la Côte dÍvoire*' (Traveaux et Documents de IRSTOM, Paris)

[11] Neuwinger, H.D. (Ed.): '*African traditional medicine – a dictionary of plant use and applications*' (Medpharm Scientific Publishers, Stuttgart, 1974), p. 173

[12] Irvine, F.R.: '*Woody plants of Ghana*' (Oxford University Press)

[13] Akendengué, B., Louis, A.M.: 'Medicinal plants used by the Masango people in Gabon', *J. Ethnopharmacol.*, 1994, **41**, (3), pp. 193–200

[14] Addy, M.E.: 'Several chromatographically distinct components from *Desmodium adscendens* inhibit smooth muscle contractions', *Int. J. Crude Drug Res.*, 1989, **27**, (2), pp. 81–91

[15] Addy, M.E.: 'Some secondary plant metabolites in *Desmodium adscendens* and their effects on arachidonic acid metabolism', *PLEFA*, 1992, **47**, (1), pp. 85–91

[16] McManus, O.B., Harris, G.H., Giangiacomo, K.M., *et al.*: 'An activator of calcium dependent potassium channels isolated from a medicinal herb', *Biochemistry*, 1993, **32**, (24), pp. 6128–6133

[17] Pothier, J., Ragot, J., Galand, N.: 'Planar chromatographic study of flavonoids and soyasaponins for validation of fingerprints of *Desmodium adscendens* of different origin', *J. Planar Chromatogr.*, 2006, **19**, (109), pp. 191–193

[18] Schacht, V.J., Neumann, L.V., Sandhi, S.K., *et al.*: 'Effects of silver nanoparticles on microbial growth dynamics', *J. Appl. Microbiol.*, 2012, **114**, (1), pp. 25–35

[19] Silver, S., Phung Le, T., Silver, G.: 'Silver as biocides in burn and wound dressings and bacterial resistance to silver compounds', *J. Ind. Microbiol. Biotechnol.*, 2006, **33**, (7), pp. 627–634

[20] Chen, X., Schluesener, H.J.: 'Nanosilver: a nanoproduct in medical application', *Toxicol. Lett.*, 2008, **176**, (1), pp. 1–12

[21] Iravani, S.: 'Green synthesis of metal nanoparticles using plants', *Green Chem.*, 2011, **13**, (10), pp. 2638–2650

[22] Ahmad, N., Sharma, S., Singh, V.N., *et al.*: 'Biosynthesis of silver nanoparticles from *Desmodium triflorum*: a novel approach towards weed utilization', *Biotechnol. Res. Int.*, 2011, **2011**, pp. 1–8

[23] Dauthal, P., Mukhopadhyay, M.: '*In vitro* free radical scavenging activity of biosynthesized gold and silver nanoparticles using *Prunus armeniaca* (apricot) fruit extract', *J. Nanopart. Res.*, 2013, **15**, (1), pp. 1366–1377

[24] Eloff, J.N.: 'A sensitive and quick microplate method to determine the minimal inhibitory concentration of plant extracts for bacteria', *Planta Med.*, 1998, **64**, (8), pp. 711–713

[25] NCCLS: 'Performance standards for antimicrobial disk susceptibility tests'. Approved standard, 8th ed. NCCLS Document M2-A8 (NCCLS, Wayne, PA, 2003)

[26] Jorgensen, J.H., Turnidge, J.D.: 'Susceptibility test methods: dilution and disk diffusion methods', in Murray, P.R., Baron, E.J., Jorgensen, J.H., *et al.* (Eds.): '*Manual of clinical microbiology*' (ASM Press, Washington, DC, 2007, 9th edn.), pp. 1152–1172

[27] Sangster, A.W., Stuart, K.L.: 'Ultraviolet spectra of alkaloids', *Chem. Rev.*, 1965, **65**, (1), pp. 69–130

[28] Mabry, T.J., Markham, K.R., Thomas, M.B.: '*The systematic identification of flavonoids*' (Springer-Verlag, Heidelberg, 1970)

[29] Vigneshwaran, N., Ashtaputre, N.M., Varadarajan, P.V., *et al.*: 'Biological synthesis of silver nanoparticles using the fungus *Aspergillus flavus*', *Mat. Lett.*, 2007, **61**, (6), pp. 1413–1418

[30] Fabry, W., Okemo, P.O., Ansorg, R.: 'Antibacterial activity of East African medicinal plants', *J. Ethnopharmacol.*, 1998, **60**, (1), pp. 79–84

[31] Bueno, J.: 'In vitro antimicrobial activity of natural products using minimum inhibitory concentrations: looking for new chemical entities or predicting clinical response', *Med. Arom. Plants*, 2012, **1**, pp. 1–7

[32] Gibbons, S.: 'Anti-staphylococcal plant natural products', *Nat. Prod. Rep.*, 2005, **21**, (2), pp. 263–277

[33] Rios, J.L., Recio, M.C.: 'Medicinal plants and antimicrobial activity', *J. Ethnopharmacol.*, 2005, **100**, (1), pp. 80–84

[34] Raveendran, P., Fu, J., Wallen, S.L.: 'Completely 'green' synthesis and stabilization of metal nanoparticles', *J. Am. Chem. Soc.*, 2003, **125**, (46), pp. 13940–13941

[35] Eustis, S., El-Sayed, M.A.: 'Why gold nanoparticles are more precious than pretty gold: noble metal surface plasmon resonance and its enhancement of the radiative and nonradiative properties of nanocrystals of different shapes', *Chem. Soc. Rev.*, 2006, **35**, (3), pp. 209–217

[36] Pandey, S., Mewada, A., Thakur, M., *et al.*: 'Rapid biosynthesis of silver nanoparticles by exploiting the reducing potential of Trapa bispinosa peel extract', *J. Nanosci.*, 2013, **2013**, pp. 1–9

[37] El-Rafie, M.H., Shaheen, T.I., Mohamed, A.A., *et al.*: 'Bio-synthesis and applications of silver nanoparticles onto cotton fabrics', *Carbohydr. Polym.*, 2012, **90**, (2), pp. 915–920

[38] Gurunathan, S., Kalishwaralal, K., Vaidyanathan, R., *et al.*: 'Biosynthesis, purification and characterization of silver nanoparticles using *Escherichia coli*', *Colloid Surf. B*, 2009, **74**, (1), pp. 328–335

[39] Shiv Shankar, S., Ahmad, A., Sastry, M.: 'Geranium leaf assisted biosynthesis of silver nanoparticles', *Biotechnol. Prog.*, 2003, **19**, pp. 1627–1631[AQ3]

[40] Muanda, F.N., Bouayed, J., Djilani, A., *et al.*: 'Chemical composition and, cellular evaluation of the antioxidant activity of *Desmodium* adscendens leaves', *J. Evid. Based Complement. Altern. Med.* 2011, **2010**, pp. 1–9

[41] Baiocchi, C., Medana, C., Giancotti, V., *et al.*: 'Qualitative characterization of *Desmodium* adscendens constituents by high-performance liquid chromatography-diode array ultraviolet-electrospray ionization multistage mass spectrometry', *Eur. J. Mass Spectrom.*, 2013, **19**, pp. 1–15

[42] O'Brien, C.: 'Physical and chemical characteristics of Aloe gels'. MSc dissertation, University of Johannesburg, Johannesburg, 2005

[43] Sathishkumar, M., Sneha, K., Won, S.W., *et al.*: '*Cinnamon zeylanicum* bark extract and powder mediated green synthesis of nano-crystalline silver particles and its bactericidal activity', *Colloid Surf. B*, 2009, **73**, (2), pp. 332–338

[44] Ravindra, S., Murali Mohan, Y., Narayana, N., *et al.*: 'Fabrication of antibacterial cotton fibres loaded with silver nanoparticles *via* 'Green approach'', *Colloid Surf. A*, 2010, **367**, (1), pp. 31–40

[45] Wan, Y., Guo, Z., Jiang, X., *et al.*: 'Quasi-spherical silver nanoparticles: aqueous synthesis and size control by the seed-mediated Lee–Meisel method', *J. Colloid Interface Sci.*, 2013, **394**, pp. 263–268

[46] Andrews, H.J., Evans, D.M.: '*Bacillus cereus* wound infections', *J. Clin. Pathol.*, 1979, **32**, (12), p. 1305

[47] Giacometti, A., Cirioni, O., Schimizzi, A.M., *et al.*: 'Epidemiology and microbiology of surgical wound infections', *J. Clin. Microbiol.*, 2000, **38**, (2), pp. 918–922

[48] Feng, Q.L., Wu, J., Chen, G.Q., *et al.*: 'A mechanistic study of the antibacterial effect of silver ions on Escherichia coli and Staphylococcus aureus', *J Biomed. Mater. Res.*, 2000, **52**, pp. 662–668

[49] Taglietti, A., Diaz Fernandez, Y.A., Amato, E., *et al.*: 'Antibacterial activity of glutathione-coated silver nanoparticles against gram positive and gram negative bacteria', *Langmuir*, 2012, **28**, pp. 8140–8148

[50] Dror-Ehre, A., Mamane, H., Belenkova, T., *et al.*: 'Silver nanoparticle–*E. coli* colloidal interaction in water and effect on *E. coli* survival', *J. Colloid Interface Sci.*, 2009, **339**, (2), pp. 521–526

[51] Albanes, A., Tang, P.S., Chan, W.C.W.: 'The effects of nanoparticle size, shape and surfaces chemistry on biological systems', *Annu. Rev. Biomed. Eng.*, 2012, **14**, pp. 1–16